Journal of Medicinal Chemistry

Article

pubs.acs.org/jmc

Fluorescein Hydrazones as Novel Nonintercalative Topoisomerase Catalytic Inhibitors with Low DNA Toxicity

A. F. M. Motiur Rahman,*[,†] So-Eun Park,[‡] Adnan A. Kadi,[†] and Youngjoo Kwon*[,‡]

[†]Department of Pharmaceutical Chemistry, College of Pharmacy, King Saud University, Riyadh 11451, Saudi Arabia

[‡]College of Pharmacy, Graduate School of Pharmaceutical Sciences, Ewha Womans University, Seoul 120-750, Republic of Korea

Supporting Information

ABSTRACT: Fluorescein hydrazones (**3a**−**3l**) were synthesized in three steps with 86−91% overall yields. Topo I- and IIα-mediated relaxation and cell viability assay were evaluated. **3d** inhibited 47% Topo I (camptothecin, 34%) and 20% Topo II (etoposide 24%) at 20 μM. **3l** inhibited 61% Topo II (etoposide 24%) at 20 μM. **3d** and **3l** were further evaluated to determine their mode of action with diverse methods of kDNA decatenation, DNA−Topo cleavage complex, comet, DNA intercalating/unwinding, and Topo IIα-mediated ATP hydrolysis assays. **3d** functioned as a nonintercalative dual inhibitor against the catalytic activities of Topo I and Topo IIα. **3l** acted as a Topo IIα specific nonintercalative catalytic inhibitor. **3d** activated apoptotic proteins as it increased the level of cleaved capase-3 and cleaved PARP in a dose- and time-dependent manner. The dose- and time-dependent increase of G1 phase population was observed by treatment of **3d** along with the increase of $p27^{kip1}$ and the decrease of cyclin D1 expression.

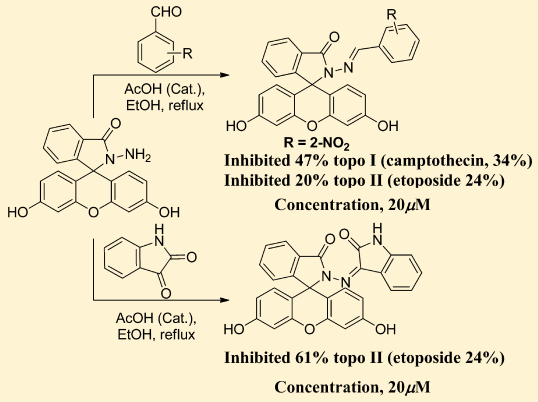

INTRODUCTION

Cancer is not just one simple disease but a complex one. The two main characteristics of cancer are uncontrolled cell growth and cell migration from the original site to distant sites in human body. Cancer is life threatening, and if the migration is not controlled, cancer can lead to death.[1] Cancerous cell proliferation is mainly related with essential process of the cell cycle (DNA synthesis, mitosis, and cytokinesis) which is controlled by several cell-cycle controlling proteins.[2,3] Among these proteins, topoisomerases have been focused by many researchers as an attractive drug target for therapeutic intervention on cancerous cell proliferation.[4,5] Two types of isomers of topoisomerase exist in humans, type I of topoisomerase (Topo I) and type II of topoisomerase (Topo II). Both are nuclear enzymes essential to resolve topological problems which unavoidably occur during DNA replication and cell division.[4,6] Topo I cuts one strand of a DNA double helix to pass the other strand through the cut and then reseals the Topo I-mediated cut, while Topo II cleaves both strands of one DNA duplex to let the other noncleaved duplex pass through a transiently formed Topo II-mediated break and then followed by religating the cleaved strands. The differences of Topo II from Topo I beside simultaneous cleavage of double strands are (i) Topo II functions in a form of homodimer with requirement of divalent metal ion, Mg^{2+}, binding and ATP hydrolysis for enzyme turn over and rapid kinetics; (ii) only Topo II enables chromosomes to be disentangled and decatenated during DNA replication by introducing transient double strand breaks.[3−7]

Topo inhibitors are grouped two types such as Topo poisons and catalytic inhibitors based on their mode of action. Topo poison is defined for compounds which stabilize the Topo−DNA complex formed transiently and covalently, known as "cleavable complex", and prevent the cleaved DNA strand(s) from religation, thus leading to an accumulation of undesired truncated DNA. Topo poison is named due to severe DNA damage and genetic toxicity induced by the Topo-mediated undesired DNA truncation. The rest of the Topo inhibitors besides Topo poisons can be grouped as a Topo catalytic inhibitor.[4,5,8,9]

Fluorescein is a synthetic organic compound having open/cyclic form (**1**, Figure 1), it is dark orange/red powder in color, soluble in water as well as in alcohol. It was first synthesized from phthalic anhydride and resorcinol in 1871 via Friedel−Craft reaction in the presence of zinc chloride.[10] Later on, a

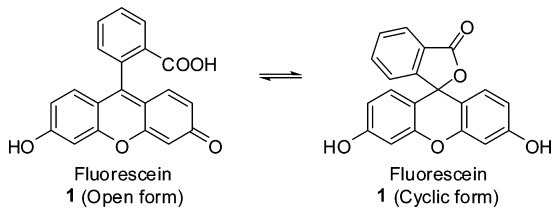

Figure 1. Structures of fluorescein.

Received: August 18, 2014

   dx.doi.org/10.1021/jm501263m | J. Med. Chem. XXXX, XXX, XXX−XXX

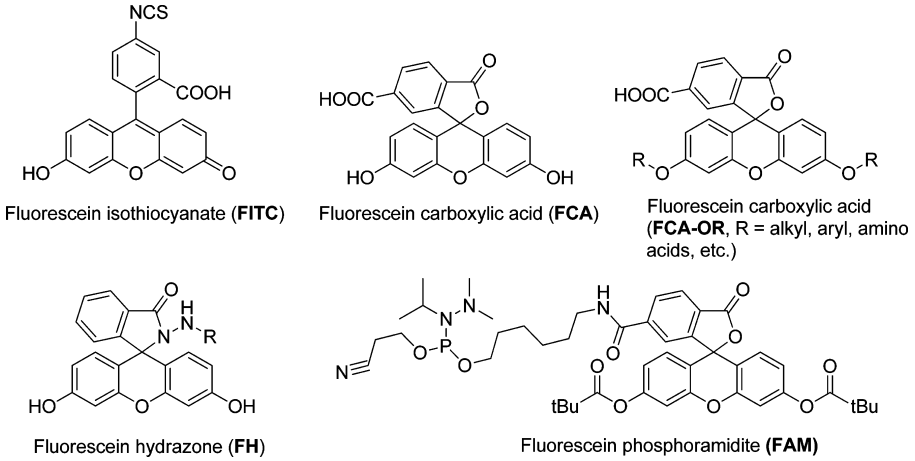

Figure 2. Structure of functionalized fluoresceins.

Scheme 1. Synthetic Scheme of Fluorescein Hydrazide (2)

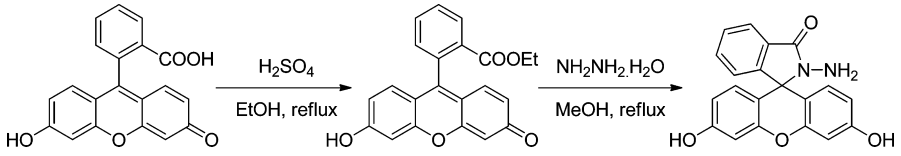

synthetic method was developed for synthesizing fluorescein by using methansulfonic acid as milder reagent and obtained high yield.[11] Fluorescein commonly used as a fluorescent tracer in microscopy, a type of dye laser, and in forensics and serology to detect latent blood stains.

Fluorescein (**1**) has been derivatized and/or functionalized particularly on the top ring with an isothiocyanate (−N═C═S) group named fluorescein isothiocyanate (FITC, Figure 2). FITC has been widely utilized as diverse forms to understand various physicochemical, photophysical, and biological implications; FITC-labeled PEO−PCL−PEO triblock copolymer,[12] FITC−deacetylated chitin conjugates,[13] FITC-labeled human plasma,[14] FITC-labeled collagen,[15] FITC−PEO conjugate,[16] FITC−cyclodextrin conjugates,[17] FITC−fullerol conjugates,[18] insulin−fluorescein conjugates,[19] bifunctional polyacrylamides containing vancomycin and fluorescein,[20] a fluorescein−ruthenium−octa-arginine conjugate,[21] lithocholyl−lysyl−fluorescein conjugates,[22] dimethylamionapthamide−fluorescein conjugates,[23] FITC-labeled lectin,[24] FITC labeling at the 5′-end of DNA with intercalating compound conjugates,[25] and FITC−dextran conjugates.[26]

Fluorescein also functionalized on the top ring with a carboxylic acid group fluorescein carboxylic acid (FCA), which has been used as precursor for the synthesis of oligonucleotides (e.g., fluorescein phosphoramidites, FAM),[27] fluorescein-tagged peptoid conjugates,[28,29] characterizing RecA−DNA interaction,[30] fluorescein-*C*-and *O*-glycosides,[31] fluorescein labeled 7-methylguanosinemonophosphate,[32] and ifenprodil conjugates.[33]

The two hydroxyl groups on the bottom of **1** have been also functionalized as hydroxyl group protected fluorescein carboxylic acid (FCA-OR) and evaluated their various properties including the detection of the esterase activity of trace copper(II),[34] fluorescent derivatizing reagent,[35] fluorescein dye,[36] fluorescent reagents in food samples,[37] a tool for determining the hydrolytic properties of fluorescein esters,[38] hydrolysis studies,[39] artificial photosynthesis and solar energy conversion,[40] and the conjugate addition of amino acid side chains.[41] In addition, fluorescein tetracysteine-tagged protein conjugates linked with a diethylamine moiety was applied to purify tetracysteine-tagged proteins[42] and fluorescein hydrazide/hydrazone was utilized as a colorimetric logic chemosensor for pH and Cu(II) ion detection.[42−46]

Although fluorescein and fluorescein derivatives/conjugates have diverse physicochemical, photophysical, and biological properties, their physiological activity and relevance to drug development still need to be clarified. A detailed search gave us the information that fluorescein derivatives derived from cyclic form of **1** (Figure 1, cyclic form) have been studied for the detection of membrane-bound DNA,[47] detection of damaged nucleic acids,[48] measurement of mammalian phosphoinositide-specific phospholipase C activity,[49] and proteolytic activities[50] rather than the open form of **1** (Figure 1, open form). In addition, fluorescein−naringenin conjugates shows 20% of the activity of naringenin.[51] It should be noted that, recently, halogenated fluorescein analogues was reported with potent microbial activity.[52] As a part of our research finding biologically active molecules for potential oncology therapeutics, we have designed a number of derivatives of fluorescein hydrazone (FH) containing no free carboxylic acid groups as stated below. To the best of our knowledge, no report has been made for the evaluation on cytotoxicity and topoisomerase activity for the fluorescein hydrazones.

RESULTS AND DISCUSSION

Chemistry. Esterification of **1** was carried out in the presence of catalytic amount of concentrate sulfuric acid in ethanol to afford fluorescein ethyl ester (FLEt) in an excellent yield (93%). The resulting ester was then refluxed with excess amount of hydrazine hydrate in methanol to lead to the desired fluorescein hydrazide (**2**) and obtained 99% yield. Compound **2** also can be prepared directly form **1** by refluxing in the

dx.doi.org/10.1021/jm501263m | J. Med. Chem. XXXX, XXX, XXX−XXX

Scheme 2. Synthetic Scheme Fluorescein Hydrazone Derivatives (3a−3l)

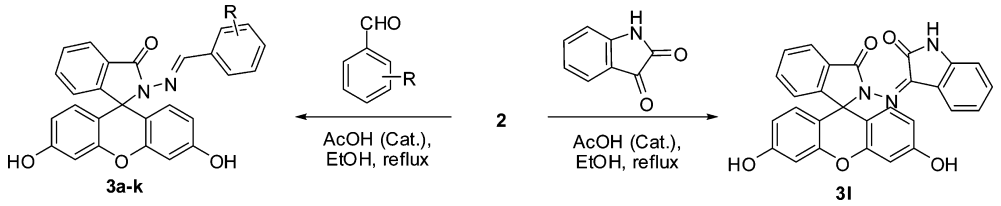

Chart 1. Structures of Synthesized Fluorescein Hydrazone Derivatives (3a−3l)

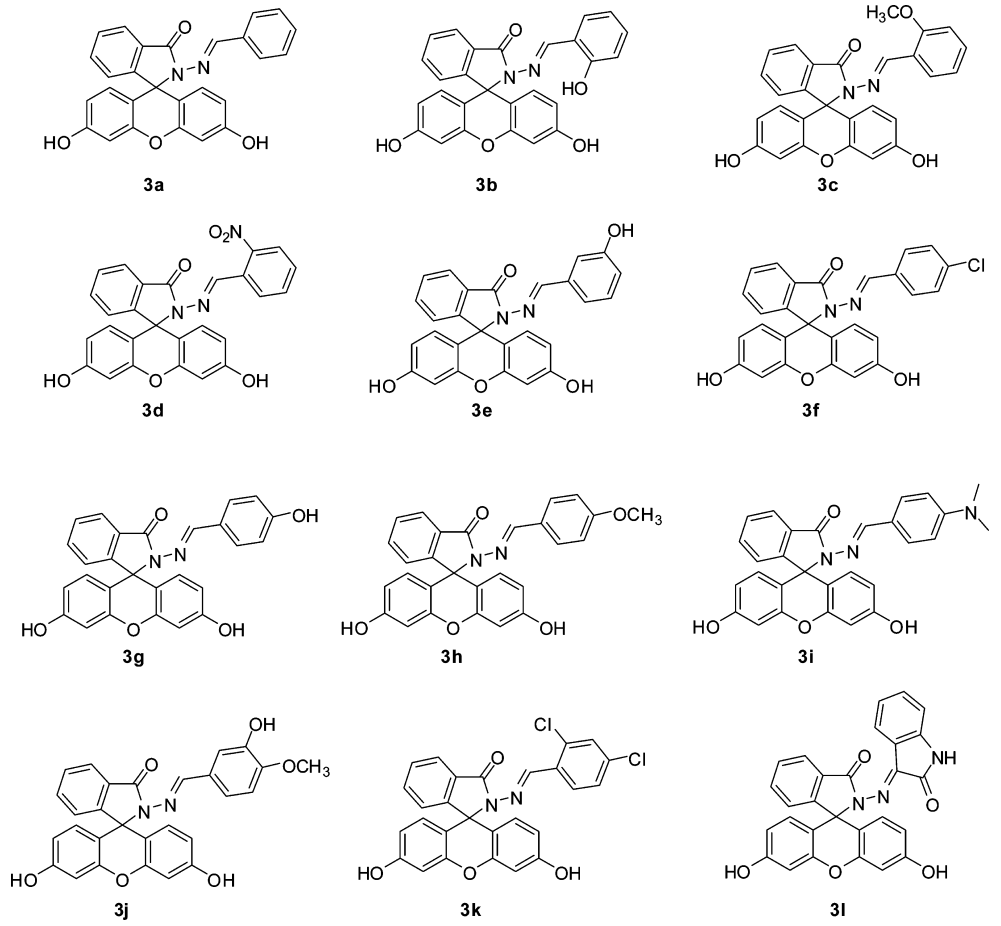

presence of excess amount of hydrazine hydrate in methanol gave 80−90% yield (Scheme 1).

Synthesis of **3a−3l** was straightforward as shown in Scheme 2. Reactions of **2** with substituted benzaldehydes were carried out in the presence of a catalytic amount of acetic acid in ethanol under refluxing conditions to afford the corresponding **3a−3k** in excellent yields (95−99%). To obtain **3l**, hydrazide **2** was refluxed with isatin in similar fashion of which the yield was 98%. It should be noted that while condensing **2** with substituted benzaldehydes in ethanol without acetic acid no products and/or byproducts were obtained even in refluxing condition for 2 days. After addition of a catalytic amount (1−3 drops) of glacial acetic acid, we obtained excellent yields (95−99%). The yield and the purity of each compound were given in Experimental Section. All the synthesized compounds are listed in Chart 1.

Topo I and II Inhibitory Activities of Compounds 3a−3l. Most tested compounds had no Topo I inhibitory activity at 100 μM treatment except for compounds **3d** and **3i** (Table 1 and Figure 3). Compounds **3d** and **3i** inhibited Topo I activity at 100 μM by 66% and 45%, respectively. Moreover, compound **3d** inhibited Topo I more strongly (47%) than camptothecin (34%) at 20 μM concentration. Most of the compounds displayed stronger Topo II inhibitory activity at 100 and 20 μM, except for compound **2**. Compounds **3f** (38%), **3k** (79%), and **3l** (61%) exhibited stronger Topo II inhibitory activities than etoposide (24%) at 20 μM concentration.

Structure−Activity Relationships (SARs) Study of 3a−3l Based on Topoisomerases Activities. Synthesized fluorescein hydrazone containing a 2-nitro group in a phenyl ring attached with fluorescein by a hydrazone bond, compound (**3d**) inhibited Topo I activity at 100 μM by 66% and at 20 μM by 47%, whereas camptothecin inhibited 34% at 20 μM concentration. While *N*,*N*-dimethyl group at the 4-position of the phenyl ring attached with fluorescein by a hydrazone bond (**3i**) decreased the inhibitory activity than **3d**, it inhibited Topo I activity at 100 μM by 45% and at 20 μM by 12%. On the other hand, containing a 2,4-dichloro (**3k**) and a isatin moiety

dx.doi.org/10.1021/jm501263m | J. Med. Chem. XXXX, XXX, XXX−XXX

Table 1. Topoisomerase I and II Inhibitory Activities of Compounds 2 and 3a−3l

	% inhibition against			
	Topo I		Topo IIα	
compd	100 μM	20 μM	100 μM	20 μM
camptothecin	52	34	NT[a]	NT
etoposide	NT	NT	82	24
2	8	NT	7	NT
3a	0	NT	80	17
3b	2	NT	76	17
3c	4	NT	74	15
3d	66	47	72	20
3e	0	NT	75	19
3f	0	NT	72	38
3g	0	NT	74	15
3h	0	NT	75	22
3i	45	16	78	21
3j	0	NT	83	19
3k	25	NT	92	79
3l	14	NT	100	61

[a]NT: nontested.

(**3l**) decrease very much inhibitory activity, its inhibited Topo I activity at 100 μM by 25% and 14%, respectively. Except above compounds (**3d**, **3i**, **3k**, and **3l**), no compounds inhibited expected Topo I activity. It should be noted that, having a 3-hydroxy group (**3e**), 4-hydroxy group (**3g**), 4-methoxy group (**3h**), and 3-hydroxy-4-methoxy groups (**3j**) did not inhibit Topo I activity at all at 100 μM concentration. All the results are summarized in Table 1.

All the compounds, **3a−3l** inhibited strong Topo II activity at 100 and 20 μM. However, having 3-hydroxy-4-methoxy groups (**3j**, 83%), 2,4-dichloro groups (**3k**, 92%), and an isatin moiety (**3l**, 100%) in the phenyl ring inhibited stronger Topo II activity at 100 μM than the etoposide (82%, Table 1). Not only that, but also at 20 μM concentration, **3k** (79%) and **3l** (61%) show much more inhibition activity than etoposide (24%).

Cell Proliferation Inhibitory Activities of Compounds 3a−3l. The cell proliferation inhibitory activities of compounds are listed in Table 2 as values of IC_{50}. Most of the tested compounds, except for compound **2**, displayed antiproliferation activity against all tested cancer cell lines. Compound **3d** displayed the highest cytotoxicity against the HCT15 cells (1.59 ± 0.05 μM). Compounds **3d** and **3l** were chosen for further study because compound **3d** was a Topo I and Topo II dual inhibitor with the strongest antiproliferative activity among tested compounds, and compound **3l** inhibited Topo II specifically.

Inhibitory Activity of Compounds 3d and 3l on Topo IIα-Mediated Decatenation of Kinetoplast DNA. The decatenation assay is suitable for screening Topo II specific inhibitor because kinetoplast DNA (kDNA) can be decatenated by Topo II but not by Topo I.[53] Compound **3d** inhibited the decatenation activity of Topo II at 50 and 100 μM by 29% and 88%, respectively (Figure 4A,C). Treatment of compound **3l** with 50 μM did not inhibit the decatenation (data not shown), therefore the concentration of compound **3l** was increased to 100 and 200 μM, which inhibited the decatenation by 46% and 91%, respectively (Figure 4B,D). However, the inhibitory activity of compound **3l** on Topo II-mediated DNA relaxation was more potent than **3d** at both treated concentrations. Ellipticine, used as a positive control, is a well-known DNA intercalating and DNA binding Topo II inhibitor. The extent of inhibition on Topo II-mediated decatenation of kDNA by ellipticine is similar to that previously observed.[54] Etoposide is a well-known Topo II poison due to its function to stabilize the transiently formed Topo II−DNA covalent complex.[4,5] Less inhibitory activity of etoposide against Topo II-mediated decatenation than ellipticine attributed to its different mode of action from that of ellipticine.[55,56] On the basis of results of relaxation and decatenation assays, both of compounds **3d** and **3l** were confirmed to inhibit potently Topo II.

Compound 3d As a Nonintercalative Catalytic Topo I and II Dual Inhibitor and Compound 3l As a Nonintercalative Catalytic Topo II Specific Inhibitor. Com-

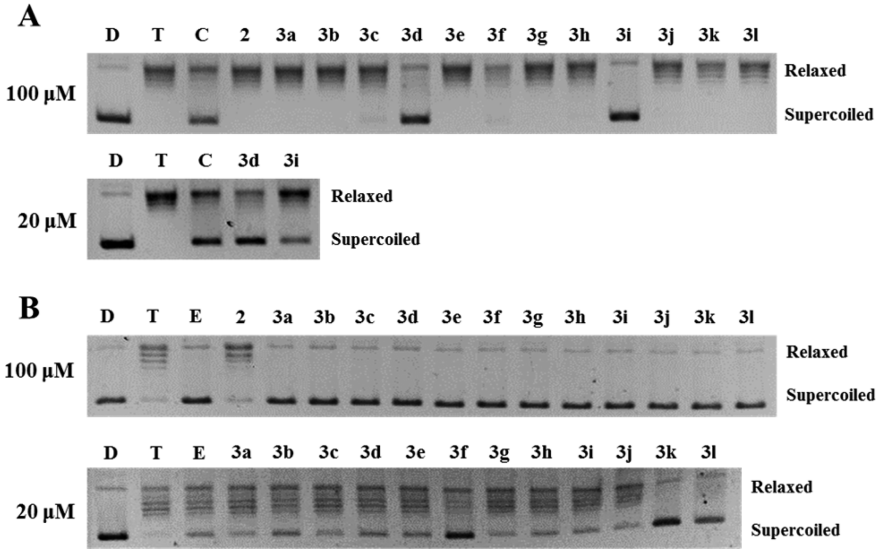

Figure 3. Topoisomerase I and IIα inhibitory activities of compounds **2** and **3a−3l**. (A) Topo I: lane D, pBR322 DNA only; lane T, pBR322 DNA + Topo I; lane C, pBR322 DNA + Topo I + camptothecin; lanes 2 and 3a−3l, pBR322 DNA + Topo I + compounds **2** and **3a−3l**. (B) Topo IIα: lane D, pBR322 DNA only; lane T, pBR322 DNA + Topo IIα; lane E, pBR322 DNA + Topo IIα + etoposide; lanes 2 and 3a−3l, pBR322 DNA + Topo IIα + compounds **2**, **3a−3l**.

dx.doi.org/10.1021/jm501263m | J. Med. Chem. XXXX, XXX, XXX−XXX

Table 2. Cell Proliferation Inhibitory Activities of Compounds 2 and 3a−3l[a]

	IC_{50} (μM)			
compd	T47D	HCT15	DU145	HEK293
adriamycin	0.57 ± 0.18	2.03 ± 2.19	0.88 ± 0.16	3.07 ± 1.67
etoposide	3.26 ± 1.54	4.46 ± 0.93	9.29 ± 0.71	6.48 ± 3.22
camptothecin	1.21 ± 0.76	0.29 ± 0.12	1.05 ± 0.69	0.12 ± 0.02
2	>50	>50	>50	>50
3a	5.28 ± 0.05	5.48 ± 0.06	7.87 ± 0.04	2.81 ± 0.03
3b	6.26 ± 0.06	6.06 ± 0.06	7.46 ± 0.03	2.38 ± 0.01
3c	>50	>50	12.35 ± 0.24	1.46 ± 0.01
3d	12.13 ± 0.03	1.59 ± 0.05	11.78 ± 0.43	4.28 ± 0.11
3e	7.61 ± 0.10	5.78 ± 0.05	9.09 ± 0.04	1.46 ± 0.01
3f	3.48 ± 0.10	5.25 ± 0.07	7.94 ± 0.17	4.74 ± 0.10
3g	11.26 ± 0.03	9.55 ± 0.01	18.49 ± 0.04	15.42 ± 0.19
3h	5.00 ± 0.08	3.99 ± 0.25	9.78 ± 0.25	13.79 ± 0.27
3i	6.53 ± 0.02	23.57 ± 0.70	45.25 ± 3.67	18.65 ± 0.17
3j	9.60 ± 0.12	16.72 ± 0.06	19.63 ± 0.13	11.15 ± 0.16
3k	5.17 ± 0.06	22.99 ± 0.32	8.44 ± 1.00	4.12 ± 0.01
3l	21.51 ± 0.11	20.58 ± 0.23	15.89 ± 0.10	37.78 ± 0.79

[a]Each data represents mean ± SD obtained from three different experiments. Cell lines used as follows: HEK293, human embryonic kidney cell; DU145, human prostate cancer cell; HCT15, human colon cancer cell; T47D, human breast cancer cell. Positive controls used are as follows: etoposide, positive control for Topo IIα and cytotoxicity; camptothecin, positive control for Topo I and cytotoxicity; adriamycin, positive control for cytotoxicity.

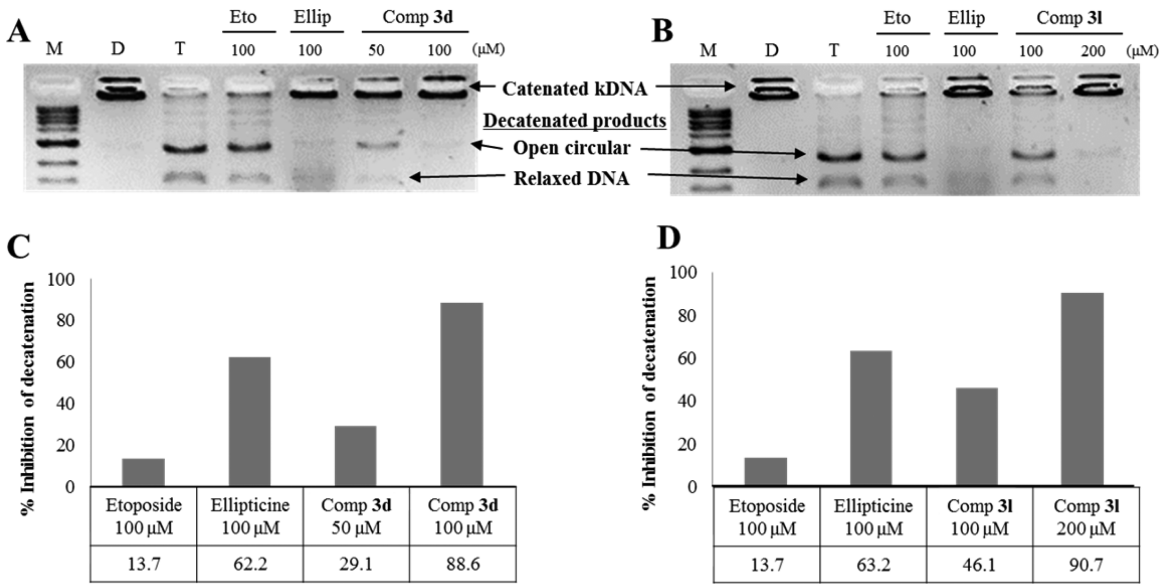

Figure 4. Compounds **3d** (A) and **3l** (B) inhibited Topo II-mediated kDNA decatenation: lane M, marker; lane D, kDNA only; lane T, kDNA + Topo IIα; lanes Eto, Ellip, and Comp **3d** and **3l**, kDNA + Topo IIα in the presence of each of compound at the designated concentration. Eto, etoposide; Ellip, ellipticine. (C,D) Quantification of decatenated products formed in (A) and (B), respectively.

pounds **3d** and **3l** were examined with cleavage complex assay whether they functioned as a Topo II poisons or catalytic inhibitor. Incubation of Topo IIα with etoposide resulted in a linear DNA band, a marker of Topo poison, as depicted in Figure 5A. However, this linear DNA band was not observed with treatment of 100 μM compounds **3d** and **3l**, even at a higher concentration of 300 μM. Therefore, we can conclude that compounds **3d** and **3l** did not stabilize the enzyme−DNA cleavage complex and did not act as classical poisons but functioned as catalytic inhibitors. To gain more insight into the fact that compounds **3d** and **3l** functioned as catalytic inhibitors, we measured DNA damage by observing comet tails using comet assay after treatment of etoposide or compounds with HCT15 cells. The comet tails occur when the stable enzyme−DNA cleavage complex is formed in cells, therefore the formation of comet tail is an important property of Topo II poisons.[57] Etoposide, used as a positive control, significantly induced DNA tails at 10 μM concentration. In contrast, compounds **3d** and **3l** did not induce at 20 μM concentration (Figure 5B,C), approving their mode of action as catalytic inhibitors. The catalytic inhibitors of Topos can be grouped into two types of intercalative and nonintercalative catalytic inhibitors.[4−6] The intercalative or nonintercalative ability of compounds **3d** and **3l** were examined with DNA intercalating/unwinding assay using a negatively supercoiled pHOT1 DNA as a substrate because the formation of supercoiled DNA in this assay is a practical characteristic of intercalative drugs.[58] Amsacrine (m-AMSA), a well-known

dx.doi.org/10.1021/jm501263m | J. Med. Chem. XXXX, XXX, XXX−XXX

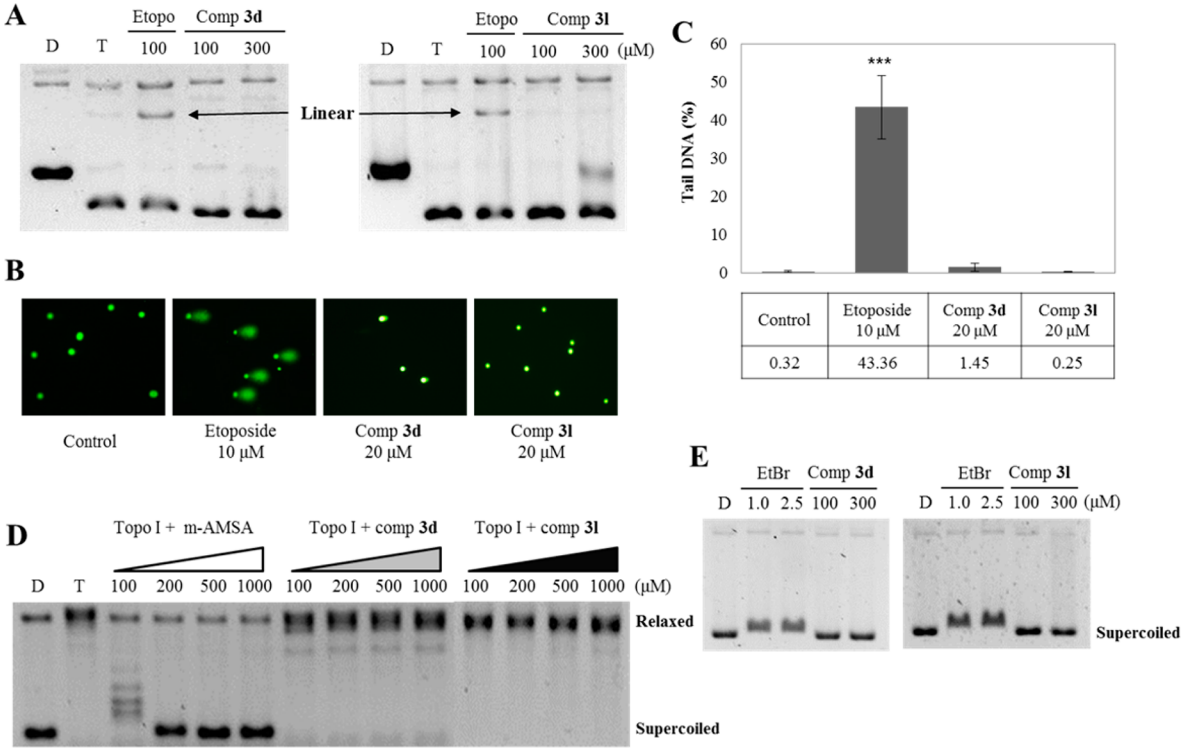

Figure 5. Compounds **3d** and **3l** functioned as nonintercalative catalytic inhibitors against Topo I/II and Topo II specifically. (A) Cleavage complex assay. In contrast to etoposide, compounds **3d** and **3l** did not induce a linear DNA band which was generated due to stabilization of a transient cleavage complex of Topo II–DNA. (B) Comet assay. Images of control (nontreated), etoposide (Topo II poison), and compounds **3d** or **3l** treated HCT15 cells. Compounds **3d** and **3l** did not induce DNA damage in HCT15 cells, but etoposide-treated HCT15 cells showed severe comet formation. (C) Graphical representation of the selected comet lengths of untreated- and treated-HCT15 cells in pixels with corresponding to concentration in (B). The percentage of tail DNA was obtained by analysis of images using Komet software. Columns and error bars indicate mean ± SD (n = 50). ***P < 0.001 significantly different from the value of control. (D) DNA intercalating/unwinding assay. m-AMSA (intercalative Topo II poison) blocked the unwinding of pHOT1 DNA, which was mediated by excess amount of Topo I and formed the supercoiled DNA in dose-dependent manner, but compounds **3d** and **3l** did not up to 1000 μM treatment. (E) DNA retardation in migration during gel electrophoresis. Ethidium bromide generated a noticeable retardation in migration of pBR322 helix DNA, but compounds **3d** and **3l** did not.

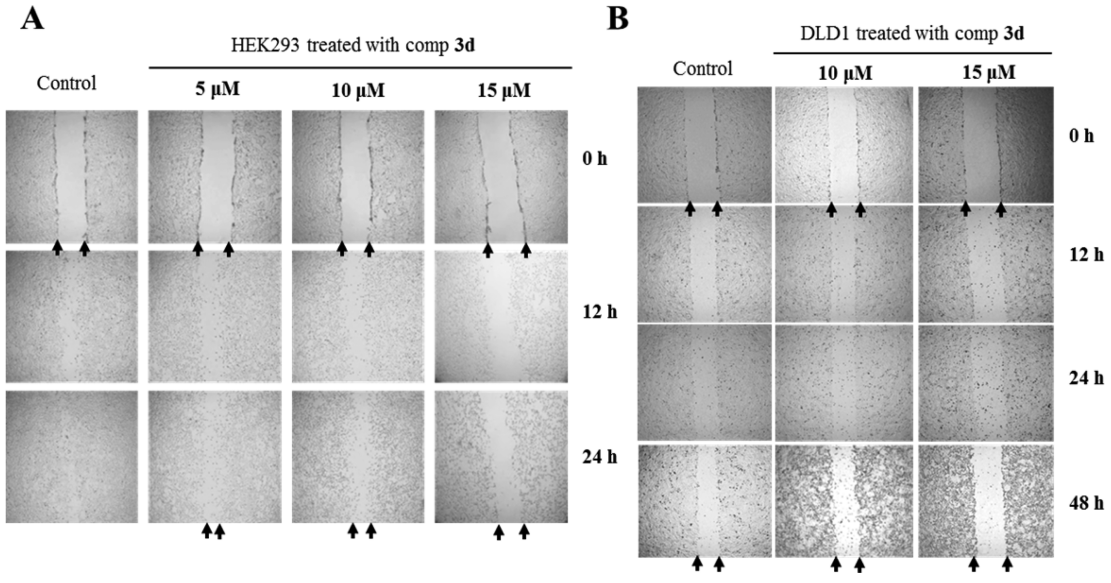

Figure 6. Compound **3d** reduced migration and proliferation of HEK293 (A) and DLD1 (B) cells. Cells were cultured in 6-well plate until reached to 90% confluence. A scratch wound in mono layer cells across the center of each well was created and followed by 4 h of serum starvation, then cells were treated with compound **3d** at designated concentrations for 24 or 48 h. The wound gap was assessed by a fluorescence inverted microscope with 5× magnification at different time points (0, 12, 24, and 48 h).

intercalative Topo II poison,[4,5] blocked unwinding of pHOT1 DNA and formed supercoiled DNA in the presence of excess Topo I in a dose-dependent manner, which is consistent with the result previously reported.[59] While compounds **3d** and **3l**

dx.doi.org/10.1021/jm501263m | J. Med. Chem. XXXX, XXX, XXX–XXX

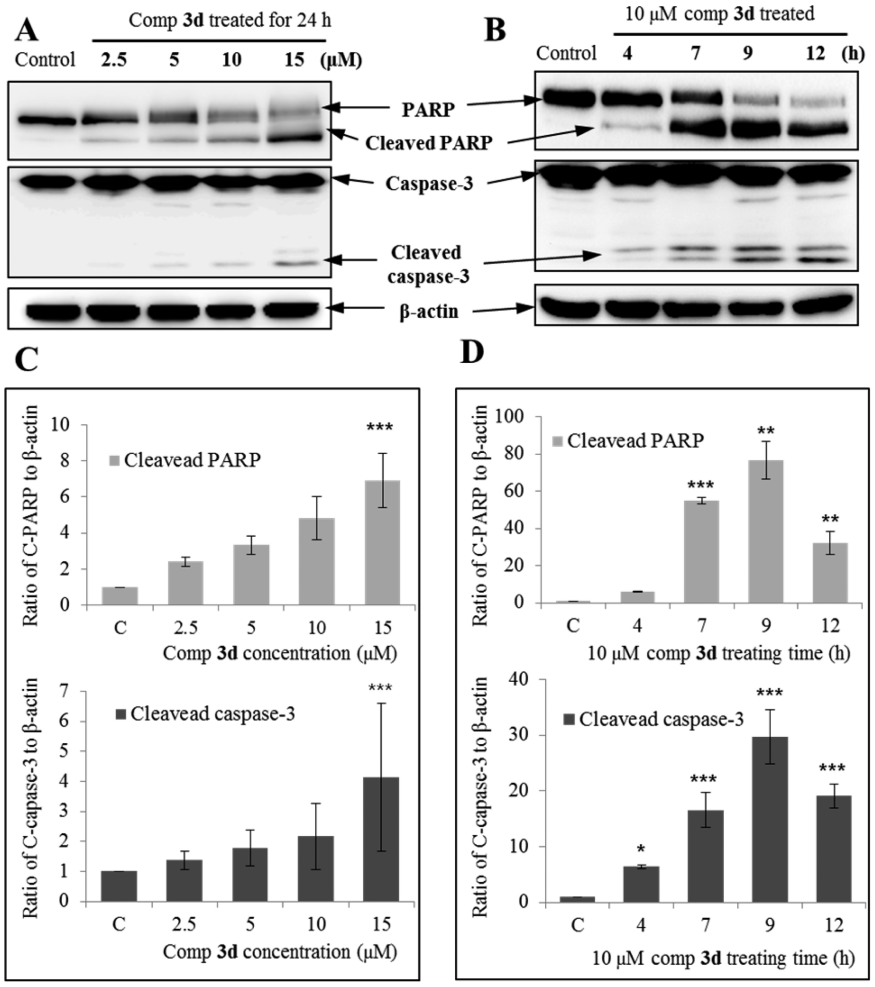

Figure 7. Compound **3d** induced apoptosis through cleaving caspase-3 and PARP in HCT15 cells. Cleaved caspase-3 and PARP were increased in HCT15 cells in a dose-dependent manner when treated with 2.5, 5, 10, and 15 μM of compound **3d** for 24 h (A) and augmented in a time-dependent manner when treated with 10 μM compound **3d** for 4, 7, 9, and 12 h (B). (C,D) The levels of proteins in (A) and (B) were normalized to β-actin and depicted as histograms. Values represent the mean ± SD obtained from three different experiments. *P < 0.05, **P < 0.01, ***P < 0.001 significantly different from the value of control (untreated).

did not block DNA unwinding at high concentration up to 1000 μM treatment (Figure 5D). In addition, the retardation of pBR322 helix DNA migration during gel electrophoresis was simply checked in the presence or absence of compounds. Ethidium bromide, a well-known DNA intercalator, induced noticeable retardation as shown in Figure 5E like the previous observation,[60] while compounds **3d** and **3l** did not. Taken together, it can be inferred that compound **3d** is a nonintercalative catalytic Topo I and II dual inhibitor and compound **3l** is a nonintercalative catalytic Topo II specific inhibitor.

Effect of Compound 3d on Migration and Proliferation in HEK293 and DLD1 Cells. As results of diverse assays performed so far, compound **3d** is inferred to be a more potent Topo inhibitor than compound **3l**. Compound **3d** demonstrated the most potent antiproliferative activity in HCT15 cells (Table 1). Therefore, HCT15 cells were chosen as a model cell line and compound **3d** was selected for further investigating its cellular mechanism. We first investigated the inhibitory activity of compound **3d** on migration and proliferation in HCT15 cells, but we failed in observing cell migration of untreated HCT15 cells. Because both HCT15 and DLD1 are human colorectal adenocarcinoma cells and derived from the same individual which are described in the cell information on ATCC and HEK293, a human embryonic kidney cell line is often used for the test of cell migration.[61,62] HEK293 and DLD1 were in this study utilized to perform a scratch wound healing assay to evaluate the effect of compound **3d** on cell migration. After a scratch wound was prepared with a sterilized microtip then the wound was checked after the treatment of 5, 10, and 15 μM compound **3d** in HEK293 cells and 10 and 15 μM in DLD1 cells, respectively. The wound gap in untreated HEK 293 cells was almost completely covered at 24 h, while cell migration was inhibited in compound **3d**-treated cells in a time and dose-dependent manner (Figure 6A). Although the anticell migratory activity of compound **3d** in DLD1 cells was slower than in HEK293 cells, DLD1 cell migration was also inhibited by compound **3d** in a time and dose-dependent manner, which confirms that compound **3d** possesses the inhibitory activity of viability and migration of cancer cells.

Compound 3d Induced Apoptosis in HCT15 Colon Cancer Cells. We observed the protein level of cleaved caspase-3 and cleaved PARP in HCT15 cells by Western blot analysis. Cleavage of caspase-3 (17 and 19 kDa), a marker of apoptotic machinery activation, was increased in a dose- and time-dependent manner when HCT15 cells were treated with

dx.doi.org/10.1021/jm501263m | J. Med. Chem. XXXX, XXX, XXX−XXX

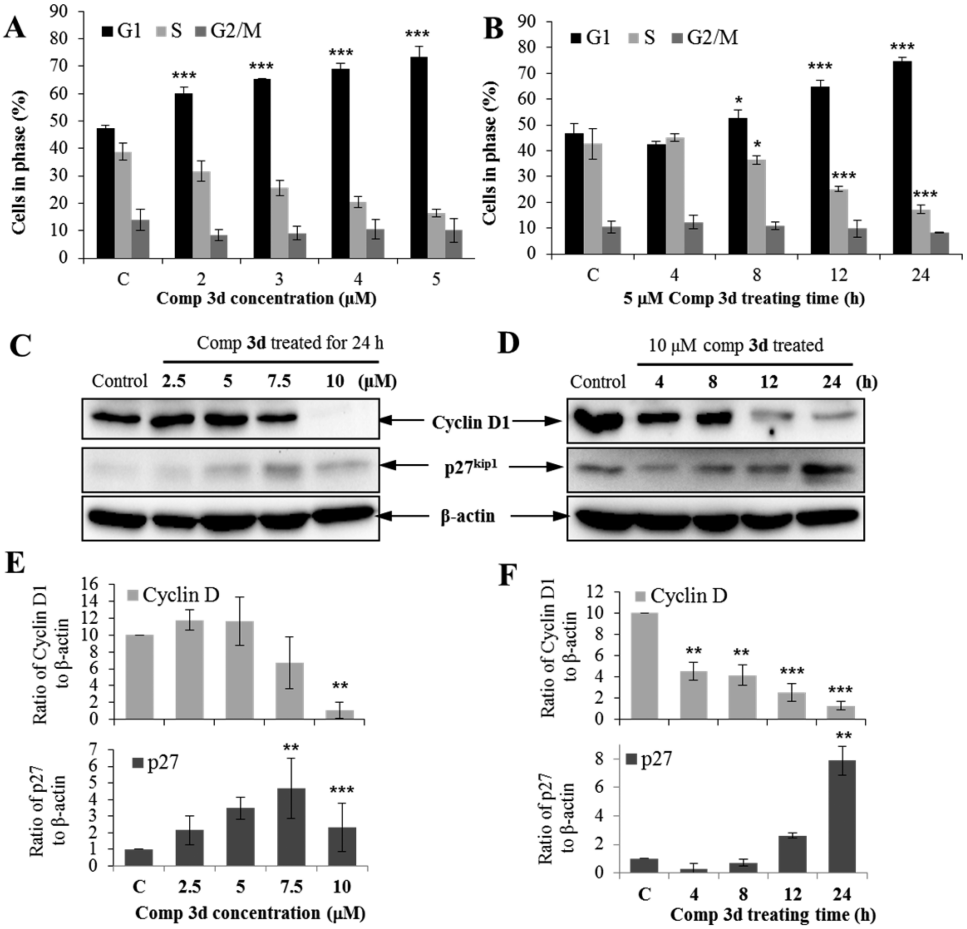

Figure 8. Treatment of compound **3d** induced G1 arrest along with an increase of $p27^{kip1}$ and a decrease of cyclin D1 in a dose- and time-dependent manner in HCT15 cells. (A,B) FACS analysis. HCT15 cells were treated with various concentrations (0, 2, 3, 4, and 5 μM) of compound **3d** for 24 h (A) and treated with 5 μM of compound **3d** for various times (0, 4, 8, 12, and 24 h) (B). Contents of compound **3d**-treated or -untreated cells (control) were depicted as histograms. Values represent the mean ± SD obtained from three different experiments. (C,D) Western analysis. The expression levels of cyclin D and $p27^{kip1}$ were detected after HCT15 cells were treated with various concentrations (0, 2.5, 5, 7.5, and 10 μM) of compound **3d** for 24 h and treated with 10 μM of compound **3d** for various times (0, 4, 8, 12, and 24 h). (E,F) The levels of proteins in (C) and (D) were normalized to β-actin. The protein level ratios of cyclin D or p27kip1 to β-actin in compound **3d**-treated or -untreated cells (control) were depicted as histograms. Values represent the mean ± SD obtained from three different experiments. $^*P < 0.05$, $^{**}P < 0.01$, $^{***}P < 0.001$ significantly different from the value of control (untreated).

2.5, 5, 10, and 15 μM compound **3d** for 24 h (Figure 7A) and treated with 10 μM compound **3d** for 4, 7, 9, and 12 h (Figure 7B). The truncation of PARP from its native 116 kDa form to 89 kDa product is also characteristic of apoptosis.[63] The expression of cleaved PARP (89 kDa) was increased in a dose- and time-dependent manner. The increment of cleaved caspase-3 and cleaved PARP indicates that compound **3d** induced apoptosis in HCT15 cancer cells.

Compound 3d Induced G1 Arrest in HCT15 Colon Cancer Cells. We examined the effect of compound **3d** on the cell cycle of HCT15 cells using a fluorescence activated cell sorter (FACS) with staining of propidium iodide. As shown in Figure 8, treatment of compound **3d** at 2, 3, 4, and 5 μM for 24 h increased G1 phase population to 60.0%, 65.3%, 69.0% and 73.4%, respectively. Greater than 1.7-fold increases in the G1 phase population was observed at 5 μM treatment of compound **3d** compared to untreated cells (Figure 8A). Furthermore, we treated HCT15 cells with 5 μM compound **3d** for 4, 8, 12, and 24 h. A significant time-dependent increase in G1 phase population was observed at treatment of 5 μM compound **3d** for 24 h (Figure 8B).

To confirm the G1 arrest effect of compound **3d**, we investigated changes in the expression of G1 checkpoint-related proteins, including cyclin D1 and $p27^{kip1}$ using Western blot analysis. The level of $p27^{kip1}$, a negative regulator of G1 progression, is increased concomitant with a decrease of cyclin D1 expression when G1 arrest is induced in cell cycles.[64,65] The protein level of cyclin D1 was significantly decreased in a dose- and time-dependent manner and reached the highest level at treatment of 10 μM compound **3d** for 24 h as shown in Figure 8C,D. The level of $p27^{kip1}$ was substantially increased in a dose- and time-dependent manner. The compound **3d**-induced G1 phase arrest was confirmed by an increase of $p27^{kip1}$ concomitant with a decrease of cyclin D1 in colon cancer cells.

CONCLUSION

Fluorescein and fluorescein derivatives or conjugates have been reported to possess diverse physicochemical, photophysical, and biological properties, however, their physiological activity and relevance to drug development are not intensively studied yet. Thirteen compounds of fluorescein hydrazones (**3a**−**3l**) were simply synthesized with excellent yields (95−99%).

dx.doi.org/10.1021/jm501263m | J. Med. Chem. XXXX, XXX, XXX−XXX

Compounds **3a**−**3l** were first evaluated by Topo I- and IIα-mediated relaxation assay and cell viability assay in several human cancer cell lines. On the basis of Topo inhibitory activity and cytotoxicity of synthesized fluorescein hydrazones (Figure 3 and Tables 1 and 2), compounds **3d** and **3l** were further evaluated to determine their mode of action with diverse methods of kDNA decatenation, DNA−Topo cleavage complex, comet, DNA intercalating/unwinding, and Topo IIα-mediated ATP hydrolysis assays (Figures 4 and 5); compound **3d** functioned as a nonintercalative dual inhibitor against the catalytic activities of Topo I and Topo IIα. Compound **3l** acted as a Topo IIα specific nonintercalative catalytic inhibitor. The effect of compound **3d** on migration and proliferation using HEK293 and DLD1 cells was further examined due to its strongest cytotoxicity and better Topo IIα-mediated kDNA decatenation efficacy than compound **3l**. Cell migration was inhibited in compound **3d**-treated cells in a dose- and time-dependent manner (Figure 6). Compound **3d** activated apoptotic proteins as it increased the level of cleaved capase-3 and cleaved PARP in a dose-and time-dependent manner (Figure 7). The dose- and time-dependent increase of G1 phase population was observed by treatment of compound **3d** along with the increase of $p27^{kip1}$ and the decrease of cyclin D1 expression (Figure 8). It is the first time a fluorescein derivative as a potent catalytic inhibitor against Topo I and IIα is reported . Taken together, compound **3d** and **3l** can be a novel scaffold for the development of antitumor agents targeting Topo I and IIα catalytic activity with a further optimizing process. Molecular docking study and in vivo experiment will be performed by our group in the very near future and the results will be explored in due course.

EXPERIMENTAL SECTION

Chemistry General. Chemicals and solvents were commercial reagent grade and were used without further purifications. All reactions were carried out under an atmosphere of nitrogen gas inside the fume hood by using a flame-dried apparatus with magnetic stirrer, unless otherwise indicated. TLC analysis was carried out on glass-backed TLC silica plates (silica gel 60 F_{254}, 0.25 mm) impregnated with fluorescence indicator (Merck art. 1.05554). The detection of UV-active substances was visualized using ultraviolet light (λ_{max} = 254 nm), and for non-UV active substances $KMnO_4$/PMA/*p*-anisaldehyde stains were used. Column chromatography was carried out on 60−120 mesh Merck silica gel. Melting points were determined on a Barnstead electrothermal digital melting point apparatus model 9100 and are uncorrected. NMR spectra were obtained using a Bruker-500 spectrometer (500 MHz for ^{1}H NMR and 125 MHz for ^{13}C NMR) and Jeol 400 MHz spectrometer and are reported as parts per million (ppm) from the internal standard of tetramethylsilane. The coupling constants *J* are reported in hertz (Hz). Peaks are described as broad signals (br), singlet (s), doublets (d), doublets of doublets (dd), doublets of doublets of doublets (ddd), triplets (t) and multiplets (m), doublets of triplets (dt), and triplets of doublets (td). Electrospray ionization (ESI) mass spectrometry (MS) experiments were performed using an Agilent high performance liquid chromatography (HPLC) 1200 connected to an Agilent 6320 ion trap mass spectrometer fitted with an electrospray ionization (ESI) ion source (Agilent Technologies, Palo Alto, CA, USA). Agilent 6300 series ion trap LC/MS system software, version 6.2, was used for data acquisition and analysis. An Eclipse Plus C18 (2.1 mm × 150 mm, 3.5 μm) column (Agilent Technologies, Palo Alto, CA, USA) was used. The mobile phase was composed of two solvents, methanol and water, with a gradient of 1−95% methanol in water, 0.3 mL/min flow rate, run time of 10 min. The ESI ion source capillary temperature was set at 325 °C; the dry gas flow rate was set to 10.0 L/min; nebulizer pressure was set to 40.00 psi; maximum accumulation time was 300000 μs; spectra were taken in positive/negative mode and scan began at 50 *m*/*z* and ended at 1000 *m*/*z*; the injection volume was 2 μL. Purity of all fluorescein hydrazones was assessed using an Eclipse Plus C18 (2.1 mm × 150 mm, 3.5 μm) column (Agilent Technologies, Palo Alto, CA, USA) in an Agilent high performance liquid chromatography (HPLC) 1200 connected to an Agilent 6320 ion trap mass spectrometer. The mobile phase was composed of two solvents, methanol and water, eluting with a gradient of 5−95% methanol in water for 10 min, flow rate of 0.3 mL/min, run time of 10 min. According to these LC−MS analyses, final compounds showed a purity of ≥98%.

Synthesis of FLEt. Fluorescein (**1**, 3.32 g, 0.01 mol) was dissolved in 50 mL of absolute ethanol, a catalytic amount of concentrate sulfuric acid was added, and the mixture was refluxed for overnight. Solvent were evaporated under vacuum, ethyl acetate was added and washed with water, 5% $NaHCO_3$, and brine and dried over anhydrous Na_2SO_4, filtered, and evaporated; the solvent obtained **FLEt** (3.35 g, 93%) as white powder; mp 241−242 °C.[66] ^{1}H NMR (CD_3OD, 500 MHz): δ, 8.30 (d, *J* = 7.0 Hz, 1H), 7.86 (t, *J* = 6.5 Hz 1H), 7.80 (t, *J* = 6.5 Hz 1H), 7.45 (d, *J* = 7.0 Hz 1H), 7.03 (d, *J* = 9.0 Hz, 1H), 6.77 (s, 2H), 7.03 (dd, *J* = 9.0, 2.0 Hz, 1H), 4.02 (q, *J* = 7.0 Hz, 1H), 0.92 (t, *J* = 7.0 Hz, 1H) ppm. ESI mass (*m*/*z*) 358.9 $[M - H]^-$ (calculated 360.10).

Synthesis of 2. Fluorescein (3.32 g, 0.01 mol) was dissolved in 50 mL of absolute ethanol, followed by the addition of hydrazine monohydrate (excess, 30 mL). The mixture was refluxed for 12 h until the fluorescence of the solution disappeared. The reaction mixture was dissolved in ethyl acetate (100 mL) then washed with water several times. The organic phase was collected, dried over anhydrous Na_2SO_4, filtered, and evaporated of the solvent. The crude product was recrystallized from methanol to give **2** (3.35 g, 99%) as white powder; R_f = 0.55 (CH_2Cl_2:methanol = 10:1); mp 272−273 °C.[43] ^{1}H NMR (CD_3OD, 500 MHz): δ, 7.89 (d, *J* = 5 Hz, 1H), 7.58−7.52 (m, 2H), 7.05 (d, *J* = 8 Hz, 1H), 6.65 (s, 2H), 6.48 (s, 4H) ppm. ^{13}C NMR (CD_3OD, 125 MHz): δ 168.6, 160.1, 154.7 153.3, 134.2, 130.5, 129.7, 129.1, 124.9, 123.8, 113.22, 110.3, 103.9, and 64.8 ppm. ESI mass (*m*/*z*) 347.0796 $[M + H]^+$, 368.9707 $[M + Na]^+$ (calculated 346.0954).

General Procedure for the Synthesis of 3a−3l.[43] A mixture of fluorescein hydrazide (**2**, 0.3 mmol) and substituted aldehyde (0.3 mmol) in 10 mL of ethanol was added a drop of glacial acetic acid, and the reaction mixture was refluxed in oil bath for 6 h. The precipitate solid was filtered, washed with cold ethanol, and air-dried to obtain **3**, which was further purified by recrystallization using methanol/dichloromethane.

*(E)-2-(Benzylideneamino)-3′,6′-dihydroxyspiro[isoindoline-1,9′-xanthen]-3-one (**3a**).* White powder (96%); mp 268−267 °C. ^{1}H NMR (CD_3OD, 500 MHz): δ 8.53 (s, 1H), 7.99 (d, *J* = 7 Hz, 1H), 7.64−7.57 (m, 2H), 7.49 (dd, *J* = 5.5, 2 Hz, 1H), 7.31 (s, 3H), 7.12 (d, *J* = 7 Hz, 1H), 6.71 (d, *J* = 2 Hz 1H), 6.54 (d, *J* = 8.5 Hz, 1H), 6.47 (dd, *J* = 8.5, 2.5 Hz, 1H) ppm. ^{13}C NMR (DMSO-d_6, 125 MHz): δ 163.6, 158.6, 152.2, 150.3, 149.2, 134.4, 134.0, 130.3, 129.1, 128.8, 128.0, 126.7, 123.8, 123.2, 112.3, 110.2, 102.4, and 65.3 ppm. LC/MS/MS: retention time: 4.9 min. ESI mass (*m*/*z*) 435.1486 $[M + H]^+$, 457.0719 $[M + Na]^+$ (calculated 434.1267).

*(E)-3′,6′-Dihydroxy-2-(2-hydroxybenzylideneamino)spiro-[isoindoline-1,9′-xanthen]-3-one (**3b**).* Yellow powder (99%); mp 325−326 °C. ^{1}H NMR (DMSO-d_6, 500 MHz): δ, 9.91 (brs, 2H), 9.18 (s, 1H), 7.90 (d, *J* = 8.2 Hz, 1H), 7.10 (pentet, *J* = 10.9 Hz, 2H), 7.43 (d, *J* = 9.2 Hz, 1H), 7.34 (t, *J* = 9.2 Hz, 1H), 7.11 (d, *J* = 9.2 Hz, 1H), 6.99 (d, *J* = 10.1 Hz 1H), 6.90 (t, *J* = 9.2 Hz, 1H), 6.64 (s, 2H), 6.46 (m, 4H) ppm. ^{13}C NMR (DMSO-d_6, 125 MHz): δ 163.4, 160.7, 158.7, 157.2, 152.2, 150.5, 150.4, 136.4, 134.1, 131.8, 129.3, 129.2, 129.0, 128.7, 128.1, 123.8, 123.2, 122.2, 119.4, 119.4, 118.8, 117.2, 116.4, 112.5, 109.4, and 62.2 ppm. LC/MS/MS: retention time: 5.1 min. ESI mass (*m*/*z*) 451.1360 $[M + H]^+$, 473.0663 $[M + Na]^+$ (calculated 450.1216).

*(E)-3′,6′-Dihydroxy-2-(2-methoxybenzylideneamino)spiro-[isoindoline-1,9′-xanthen]-3-one (**3c**).* White cream (99%); mp 297−298 °C. ^{1}H NMR (CD_3OD, 500 MHz): δ, 8.56 (s, 1H), 7.87 (d, *J* = 10.5 Hz, 1H), 7.69 (d, *J* = 7.0 Hz, 1H), 7.52−7.45 (m, 2H), 7.17 (td, *J*

dx.doi.org/10.1021/jm501263m | J. Med. Chem. XXXX, XXX, XXX−XXX

= 7.5, 1.5 Hz, 1H), 6.97 (d, J = 8.5 Hz, 1H), 6.76 (t, J = 7.0 Hz, 1H), 6.58 (d, J = 2.0 Hz 1H), 6.40 (d, J = 8.5 Hz, 1H), 6.35 (dd, J = 8.5, 2.0 Hz, 1H), 3.61 (s, 3H) ppm. ^{13}C NMR (DMSO-d_6, 125 MHz): δ 163.5, 158.5, 157.8, 152.1, 150.6, 144.1, 133.9, 131.8, 129.0, 129.0, 128.0, 124.6, 123.8, 123.1, 122.5, 120.7, 112.3, 111.9, 110.0, 102.4, 65.1, and 55.7 ppm. LC/MS/MS: retention time: 3.6 min. ESI mass (m/z) 465.1515 $[M + H]^+$, 487.1260 $[M + Na]^+$ (calculated 464.1372).

(E)-3′,6′-Dihydroxy-2-(2-nitrobenzylideneamino)spiro-[isoindoline-1,9′-xanthen]-3-one (**3d**). Yellow needle (98%); mp 287–289 °C. ^{1}H NMR (DMSO-d_6, 500 MHz): δ, 9.95 (s, 2H), 9.23 (s, 1H), 7.95 (t, J = 10.1 Hz, 2H), 7.71 (d, J = 4.5 Hz, 2H), 7.69–7.57 (m, 3H), 7.12 (d, J = 9.2 Hz, 1H), 6.66 (s, 2H), 6.52 (d, J = 11.9 Hz, 2H), 6.45 (d, J = 11 Hz, 2H) ppm. ^{13}C NMR (DMSO-d_6, 125 MHz): δ 164.2, 158.7, 152.0, 150.8, 148.0, 142.2, 134.4, 133.7, 130.8, 129.2, 128.6, 128.1, 127.8, 127.0, 124.6, 123.8, 123.4, 112.4, 109.5, 102.6, and 65.3 ppm. LC/MS/MS: retention time: 2.1 min. ESI mass (m/z) 434.1259 $[(M - NO_2) + H]^+$, 462.1417 $[(M - OH) + H]^+$, 480.0977 $[M + H]^+$, 502.0716 $[M + Na]^+$ (calculated 479.1117). LC/MS/MS: retention time: 3.7 min. ESI mass (m/z) 480.1333 $[M + H]^+$, 502.0577 $[M + Na]^+$ (calculated 479.1117).

(E)-3′,6′-Dihydroxy-2-(3-hydroxybenzylideneamino)spiro-[isoindoline-1,9′-xanthen]-3-one (**3e**). Yellowish-white cream (98%); mp 289–291 °C. ^{1}H NMR (DMSO-d_6, 500 MHz): δ, 9.93 (s, 2H), 9.59 (s, 1H), 8.89 (s, 1H), 7.92 (d, J = 7.0 Hz, 1H), 7.65–7.58 (m, 2H), 7.15 (t, J = 7.5 Hz, 1H), 7.15 (d, J = 7.5 Hz, 1H), 6.85 (s, 1H), 6.85 (s, 1H), 6.83 (d, J = 7.5 Hz, 1H), 6.76 (dd, J = 7.5, 1.5 Hz, 1H), 6.66 (d, J = 2 Hz, 2H), 6.51 (d, J = 8.5 Hz, 2H), 6.46 (dd, J = 8.5, 2 Hz, 2H) ppm. ^{13}C NMR (DMSO-d_6, 125 MHz): δ 163.7, 158.5, 157.2, 152.1, 150.6, 149.3, 135.6, 133.9, 129.9, 129.0, 128.8, 128.0, 123.7, 123.2, 118.6, 117.8, 11.3, 112.2, 110.3, 102.5, and 65.2 ppm. LC/MS/MS: retention time: 2.7 min. ESI mass (m/z) 451.1260 $[M + H]^+$, 473.0589 $[M + Na]^+$ (calculated 450.1216).

(E)-2-(4-Chlorobenzylideneamino)-3′,6′-dihydroxyspiro-[isoindoline-1,9′-xanthen]-3-one (**3f**). White powder (95%); mp 308–309 °C. ^{1}H NMR (DMSO-d_6, 500 MHz): δ, 9.93 (s, 2H), 9.10 (s, 1H), 7.93 (d, J = 7.0 Hz, 1H), 7.66–7.59 (m, 2H), 7.44 (d, J = 2.0 Hz, 4H), 7.15 (d, J = 7.5 Hz, 1H), 6.66 (d, J = 2.0 Hz, 2H), 6.50 (d, J = 8.5 Hz, 2H), 6.46 (dd, J = 8.5, 2 Hz, 2H) ppm. ^{13}C NMR (DMSO-d_6, 125 MHz): δ 163.7, 158.6, 152.2, 150.3, 147.9, 134.8, 134.1, 133.3, 129.1, 128.9, 128.3, 128.0, 123.8, 123.2, 112.3, 110.1, 102.5, and 65.4 ppm. LC/MS/MS: retention time: 6.2 min. ESI mass (m/z) 469.1834 $[M(^{35}Cl) + H]^+$, 470.9947 $[M(^{37}Cl) + H]^+$ (calculated 468.0877).

(E)-3′,6′-Dihydroxy-2-(4-hydroxybenzylideneamino)spiro-[isoindoline-1,9′-xanthen]-3-one (**3g**). Yellowish-white cream (97%); mp 281–283 °C. ^{1}H NMR (DMSO-d_6, 500 MHz): δ, 9.93 (s, 2H), 8.93 (s, 1H), 7.89 (d, J = 6.5 Hz, 1H), 7.60 (pentet, J = 8.5 Hz, 2H), 7.26 (d, J = 8.5 Hz, 2H), 7.10 (d, J = 7.0 Hz, 1H), 6.73 (d, J = 8.5 Hz, 2H), 6.64 (d, J = 1.5 Hz, 2H), 6.49 (d, J = 8.5 Hz, 2H), 6.46 (dd, J = 8.5, 2 Hz, 2H) ppm. ^{13}C NMR (DMSO-d_6, 125 MHz): δ 163.3, 159.7, 158.4, 152.2, 150.4, 133.6, 129.2, 129.0, 128.6, 128.0, 125.3, 123.6, 123.0, 115.7, 112.2, 110.3, 102.4, and 65.2 ppm. LC/MS/MS: retention time: 2.4 min. ESI mass (m/z) 451.1226 $[M + H]^+$ (calculated 450.1216).

(E)-3′,6′-Dihydroxy-2-(4-methoxybenzylideneamino)spiro-[isoindoline-1,9′-xanthen]-3-one (**3h**). White cream (99%); mp 274–275 °C. ^{1}H NMR (DMSO-d_6, 500 MHz): δ, 9.90 (s, 2H), 9.03 (s, 1H), 7.91 (d, J = 7.0 Hz, 1H), 7.65–7.58 (m, 2H), 7.38 (d, J = 8.5 Hz, 2H), 7.13 (d, J = 7.0 Hz, 1H), 6.93 (d, J = 8.5 Hz, 2H), 6.65 (d, J = 1.5 Hz, 2H), 6.49 (d, J = 8.5 Hz, 2H), 6.46 (dd, J = 8.5, 2 Hz, 2H), 3.75 (s, 3H) ppm. ^{13}C NMR (DMSO-d_6, 125 MHz): δ 163.4, 161.0, 160.8, 158.5, 152.2, 150.3, 149.7, 133.8, 129.3, 129.0, 128.6, 128.1, 127.0, 123.7, 123.1, 114.3, 112.2, 110.3,102.4, 65.3, and 55.2 ppm. LC/MS/MS: retention time: 3.8 min. ESI mass (m/z) 465.2472 $[M + H]^+$, 487.1383 $[M + Na]^+$ (calculated 464.1372).

(E)-3′,6′-Dihydroxy-2-(4-(dimethylamino)benzylideneamino)-spiro[isoindoline-1,9′-xanthen]-3-one (**3i**). Yellow powder (99%); mp 316–317 °C. ^{1}H NMR (DMSO-d_6, 500 MHz): δ, 9.90 (s, 2H), 8.91 (s, 1H), 7.88 (d, J = 6.0 Hz, 1H), 7.59 (t, J = 7.5 Hz, 2H), 7.25 (d, J = 8.0 Hz, 2H), 7.11 (d, J = 6.0 Hz, 1H), 6.64 (overlapped, 4H), 6.48 (overlapped, 4H), 2.91 (s, 6H) ppm. ^{13}C NMR (DMSO-d_6, 125 MHz): δ 163.5, 158.9, 152.8, 150.2, 151.8, 150.8, 133.9, 130.1, 129.4, 128.7, 128.5, 124.1, 123.4, 122.1, 112.7, 112.1, 111.0, 102.9, 65.7, and 19.0 ppm. LC/MS/MS: retention time: 4.0 min. ESI mass (m/z) 478.2045 $[M + H]^+$ (calculated 477.1689).

(E)-3′,6′-Dihydroxy-2-(3-hydroxy-4-methoxybenzylideneamino)-spiro[isoindoline-1,9′-xanthen]-3-one (**3j**). Yellowish-white cream (95%); mp 301–303 °C. ^{1}H NMR (DMSO-d_6, 500 MHz): δ, 9.92 (s, 2H), 9.24 (s, 1H), 8.84 (s, 1H), 7.88 (d, J = 9.2 Hz, 1H), 7.59 (pentet, J = 9.2 Hz, 2H), 7.09 (d, J = 9.2 Hz, 1H), 6.90 (s, 1H), 6.88 (d, J = 11.0 Hz, 1H), 6.80 (d, J = 10.1 Hz, 1H), 6.64 (d, J = 1.9 Hz, 2H), 6.49 (d, J = 11.0 Hz, 2H), 6.43 (dd, J = 11.0, 1.8 Hz, 2H) 3.74 (s, 3H) ppm. ^{13}C NMR (DMSO-d_6, 125 MHz): δ 163.4, 158.5, 152.1, 150.6, 150.2, 150.1, 146.7, 133.7, 129.1, 129.0, 128.0, 127.2, 123.6, 123.0, 120.5, 112.3, 111.8, 110.2, 102.5, 65.2, and 56.0 ppm. LC/MS/MS: retention time: 1.6 min. ESI mass (m/z) 481.1588 $[M + H]^+$, 503.0988 $[M + Na]^+$. LC/MS/MS: retention time: 2.4 min. ESI mass (m/z) 481.1760 $[M + H]^+$, 503.1167 $[M + Na]^+$ (calculated 480.1321).

(E)-2-(2,4-Dichlorobenzylideneamino)-3′,6′-dihydroxyspiro-[isoindoline-1,9′-xanthen]-3-one (**3k**). Yellowish-white powder (95%); mp 349–350 °C. ^{1}H NMR (DMSO-d_6, 500 MHz): δ, 9.97 (s, 2H), 8.97 (s, 1H), 7.95 (d, J = 7.5 Hz, 1H), 7.69–7.60 (m, 4H), 7.44 (dd, J = 8.5, 1.5 Hz, 1H), 7.13 (d, J = 7.0 Hz, 1H), 6.67 (d, J = 2.0 Hz, 2H), 6.52 (d, J = 8.5 Hz, 2H), 6.47 (dd, J = 9.0, 2 Hz, 2H) ppm. ^{13}C NMR (DMSO-d_6, 125 MHz): δ 164.0, 158.7, 152.0, 150.9, 141.0, 135.3, 134.4, 133.9, 130.5, 129.3, 129.2, 128.0, 128.0, 127.0, 123.8, 123.4, 112.6, 110.1, 102.5, and 65.0 ppm. LC/MS/MS: retention time: 8.1 min. ESI mass (m/z) 503.2564 $[M(^{35}Cl) + H]^+$, 502.8 $[M(^{37}Cl) + H]^+$; (calculated 502.0487).

(E)-3′,6′-Dihydroxy-2-(2-oxoindolin-3-ylideneamino)spiro-[isoindoline-1,9′-xanthen]-3-one (**3l**). Orange solid (98%); mp 261–262 °C. ^{1}H NMR (DMSO-d_6, 500 MHz): δ, 10.87 (s, 1H), 9.94 (s, 2H), 7.98 (d, J = 9.1 Hz, 1H), 7.70–7.62 (m, 2H), 7.37 (t, J = 9.1 Hz, 1H), 7.18 (d, J = 9.2 Hz, 1H), 7.15 (d, J = 10.0 Hz, 1H), 6.99 (t, J = 9.2 Hz, 1H), 6.83 (d, J = 10.0 Hz, 1H), 6.59 (s, 2H), 6.56 (d, J = 11.0 Hz, 2H), 6.42 (dd, J = 11.0 Hz, 2H) ppm. ^{13}C NMR (DMSO-d_6, 125 MHz): δ 163.7, 159.9, 158.6, 152.1, 152.0, 151.3, 144.8, 134.3, 133.6, 129.3, 128.4, 128.2, 128.0, 124.0, 123.9, 122.4, 117.0, 112.4, 110.6, 109.8, 102.3, and 67.0 ppm. LC/MS/MS: retention time: 2.4 min. ESI mass (m/z) 476.1468 $[M + H]^+$ (calculated 475.1168).

Human Topo I and Topo IIα Relaxation Assay. Topoisomerases I and II (Topo I and II) inhibition were measured by assessing the relaxation of supercoiled pBR 322 plasmid DNA as previously described.[67] The mixture of 100 ng of supercoiled DNA pBR322 (Thermo Scientific, USA) and 1 unit of human Topo I (TopoGen, USA) or Topo IIα (USB Corp., USA) was incubated in the absence or presence of the prepared compounds at 37 °C for 1 h in the reaction buffer (Topo I, 10 mM Tris HCl (pH 7.9) containing 1 mM EDTA, 0.15 M NaCl, 0.1% BSA, 0.1 mM spermidine, and 5% glycerol; Topo IIα, 10 mM tris-HCl (pH 7.9) containing 50 mM NaCl, 50 mM KCl, 5 mM $MgCl_2$, 0.1 mM EDTA, 15 μg/mL BSA, and 1 mM ATP). The 10 μL of the reaction mixture as a final volume was terminated by adding 2.5 μL of the stop solution (Topo I, 0.5% sarcosyl containing 0.00025% bromophenol blue and 2.5% glycerol; Topo IIα, 0.7 mM EDTA). The reaction mixture was then electrophoresed on a 0.8% agarose gel at 60 V for 1 h with TAE running buffer. Gels were stained for 15 min in an aqueous solution of ethidium bromide (0.5 μg/mL). DNA bands were visualized by trans-illumination with UV light and were quantitated using an Alpha Tech Imager (Alpha Innotech Corporation). Camptothecin (Sigma, USA) and etoposide (Sigma, USA) were used as positive controls as Topo I inhibitor and Topo II inhibitors, respectively.

Cytotoxicity Assay. Cytotoxicity were evaluated using diverse cancer cell lines following the previous method.[68] HCT15 (human colon cancer cell lines), T47D (human breast cancer cell line), and DU145 (human prostate cancer cell line) were grown in RPMI1640 (Hyclone, USA), and HEK293 (human kidney embryonic cell line) was cultured in DMEM (Hyclone, USA). After seeding cells in 96-well plates at a density of 2–4 × 10^4 cells per well with incubation

dx.doi.org/10.1021/jm501263m | J. Med. Chem. XXXX, XXX, XXX–XXX

overnight in 0.1 mL of media supplemented with 10% Fetal Bovine Serum (FBS) (Hyclone, USA) in a 5% CO_2 incubator at 37 °C, culture medium in each well was exchanged with 0.1 mL aliquots of medium containing graded concentrations of each compound and incubated continuously for 72 h. Then 5 μL of the cell counting kit-8 solution (Dojindo, Japan) was added to each well and incubated for additional 4 h. The absorbance of each well was measured using an automatic ELISA reader system (Bio-Rad 3550, USA) at 450 nm. The IC_{50} values were calculated with using TableCurve (Jandel Scientific Software, USA).

kDNA Decatenation Assay. The assay was performed as following the previous method[67] in a total reaction volume of 10 μL containing 50 ng of kDNA (TopoGEn, USA), compound, and 3 units of human Topo IIα in the reaction buffer solution (10 mM tris-HCl (pH 7.9) containing 50 mM NaCl, 50 mM KCl, 5 mM $MgCl_2$, 0.1 mM EDTA, 15 μg/mL BSA, and 1 mM ATP). The reaction mixtures were incubated for 30 min at 37 °C and then terminated by the addition of 2.5 μL of stop solution containing 5% SDS, 25% ficoll, and 0.05% bromphenol blue followed by treatment with 0.25 mg/mL proteinase K (Roche) at 37 °C for 30 min to eliminate the protein. Reaction mixtures were resolved by electrophoresis on a 1.2% (w/v) agarose gel containing 0.5 μg/mL ethidium bromide in the TAE buffer. DNA bands were visualized by UV and photographed and documented with an Alpha Tech Imager.

Cleavage Complex Stabilization Assay. Supercoiled DNA pBR322 (100 ng) and 3 units of Topo IIα were mixed and incubated for 5 min at 37 °C. Compound was then added and then incubated at 37 °C for 20 min and stopped with 10% SDS, followed by digestion with proteinase K at 45 °C for 30 min.[67] After the addition of the loading buffer, the reaction mixture was heated for 2 min at 70 °C and then electrophoresed on a 0.8% agarose gel in TAE buffer containing 0.5 μL/mL ethidium bromide at 20 V for 6 h. The gel was destained with water for 10 min and visualized by an Alpha Tech Imager.

Comet Assay. Comet assay was performed using the Alkaline Comet Assay kit (Trevigen, USA) according to the method previously reported.[69] HCT15 cells were seeded in a 6-well plate in a density of 10^5 cells per well with incubation for 24 h. Cells were then incubated either without or with etoposide or compound for 24 h in serum free media and harvested by trypsinization. The harvested cells were resuspended in 1 mL of ice-cold PBS. Then 8 μL of resuspended cells were mixed with 80 μL of low-melting agarose at 37 °C, followed in the same way as the previous method.[69] Comet images were captured with Zeiss HBO100 microscope illumination system (Carl Zeiss, Germany) equipped with epq100-isolated epifluorescence condenser. A total of 50 HCT15 cells were randomly analyzed with an image analysis system (Komet 5.5, Kinetic Imaging Ltd., UK). Komet 5.5 software calculated the lengths of the comet tails, and the mean values represented the extent of the DNA damage.

DNA Unwinding/Intercalating Assay. The DNA-unwinding capacity of compound was analyzed using a DNA unwinding kit (TopoGEN, USA) according to the method previously reported.[67,69] First, 100 ng of pHOT1 plasmid was treated with 4 units of Topo I in reaction buffer (10 mM Tris HCl (pH 7.9) containing 1.5 M NaCl, 1% BSA, 1 mM spermidine, and 50% glycerol) for 30 min at 37 °C. After incubation, various concentrations of m-AMSA or compounds **3d** or **3l** were added and incubated at 37 °C for an additional 30 min followed by addition of 1 μL of Topo I stop buffer. The resulting aqueous phase was then resolved on 1% agarose gels at 15 V/cm for 12−15 h. After electrophoresis, gels were stained in TAE buffer with ethidium bromide for 30 min and visualized using an Alpha Tech Imager. The compound inhibitory activity of DNA unwinding was also evaluated by monitoring retardation of DNA migration.[67] Briefly, 125 ng of negatively supercoiled DNA pBR322 and 100 or 300 μM of investigational compounds in a total volume of 10 μL was incubated at 37 °C for 20 min. Reaction mixtures were resolved on 1% agarose gels at 20 V/cm for 12−16 h. After electrophoresis, gels were stained in TAE buffer with ethidium bromide for 30 min and visualized using an Alpha Tech Imager.

Cell Migration Assay. HEK293 and DLD1 cells were cultured in a 6-well plate to 90% confluency. A clean wound in the cell monolayer cells was then created across the center of the well with a sterile microtip. After starvation with low serum media (1% FBS in DMEM) for 4 h, the cells were exposed to compound (5, 10, or 15 μM) for 24 or 48 h and allowed to migrate in the medium. The wound was assessed by a fluorescence inverted microscope with 5× magnification at different time points (0, 12, 24, and 48 h).

Western Blot Assay. HCT15 cells were grown on 60 mm tissue culture dishes at 1×10^6 cells until reaching 80% confluency. The cells were then treated with investigational compounds at various concentrations for various incubation times as designated in figure legend. Cells were lysed in lysis buffer solution containing 50 mM Tris HCl, 300 mM NaCl, 1% Triton X-100, 10% glycerol, 1.5 mM $MgCl_2$, 1 mM $CaCl_2$, 1 mM PMSF, and 1% protease inhibitor cocktail. Then 70 μg of protein per sample was resolved by 8 or 10% SDS-PAGE and transferred to a PVDF membrane (Millipore, USA). The membranes were blocked with 5% skim milk in Tris buffered saline containing 0.1% Tween 20 (TBST) and probed with primary antibodies in a dilution ratio of 1:1000 for 2−3 h. The blots were washed, exposed to HRP-conjugated antirabbit IgG (Cell Signaling Technology Inc. USA) in a dilution ratio of 1:2000 for 2 h, and detected with ECL Western blotting detection reagent (Animal Genetics Inc., Korea). All primary antibodies used were purchased from Cell Signaling Technology Inc. (USA). Western blot images were taken by LAS-3000 (Fuji Photo Film Co., Ltd., Japan) and analyzed using Multi-Gauge Software (Fuji Photo Film Co. Ltd., Japan).

FACS Analysis. HCT15 cells were seeded in 60 mm dishes at a density of 5×10^5 cells per dish. After reached 80% confluency, cells were treated with the test compounds at various concentrations for various times as designated in figure legend. Cells were then washed with ice-cold PBS (pH 7.4) and harvested by centrifugation at 2000 rpm for 5 min. The pellets were fixed with 70% ethanol, and fixed cells were then washed with PBS before incubation with 50 mg/mL propidium iodide (Sigma, USA) and 2.5 mg/mL RNase (Sigma, USA). Fluorescence was measured with a fluorescence-activated cell sorting (FACS)-Caliber flow cytometer (BD Biosciences, USA). At least 10000 cells were measured for each sample.[70]

Statistical Analysis. Data are expressed as the means ± standard deviation (SD), with each experiment performed in triplicate. Comparison of the differences was conducted with an analysis of variance (ANOVA) using the Prism statistical software package (GraphPad Software, USA). The differences were considered statistically significant when the p value was <0.05.

■ ASSOCIATED CONTENT

Ⓢ Supporting Information

Proton (^1H) and carbon (^{13}C) NMR and mass spectra of synthesized compounds. This material is available free of charge via the Internet at http://pubs.acs.org.

■ AUTHOR INFORMATION

Corresponding Authors

*For A.F.M.M.R.: phone, +966 11 46 70237; fax, +966 11 46 76220; E-mail, afmrahman@ksu.edu.sa.

*For Y.K.: phone, +82 23 277 4653; fax, +82 23 277 2851; E-mail, ykwon@ewha.ac.kr.

Notes

The authors declare no competing financial interest.

■ ACKNOWLEDGMENTS

This work is funded by research grant from the The National Plan for Science, Technology and Innovation, Kingdom of Saudi Arabia (project no. 11-MED-1909-02).

■ ABBREVIATIONS USED

FACS, fluorescence activated cell sorter; FCA, fluorescein carboxylic acid; FLEt, fluorescein ethyl ester; FH, fluorescein

hydrazone; FITC, fluorescein isothiocyanate; FITC-PEO, fluorescein isothiocyanate- poly(ethylene oxide); FAM, fluorescein phosphoramidites; FCA-OR, hydroxyl group protected fluorescein carboxylic acid; kDNA, kinetoplast DNA; PEO−PCL−PEO, poly(ethylene oxide)-*block*-poly(3-caprolactone)-*block*-poly(ethylene oxide); pHOT1 DNA, supercoiled plasmid DNA; PARP, poly(ADP-ribose) polymerase

REFERENCES

(1) Simone, J. V. *Introduction to Oncology*, 21st ed.; W. B. Saunders Company: Philadelphia, 2000; pp 1029−1032.

(2) Murray, A. W. Recycling the cell cycle. *Cell* **2004**, *116*, 221−234.

(3) Kohn, K. W. Molecular interaction map of the mammalian cell cycle control and dna repair systems. *Mol. Biol. Cell* **1999**, *10*, 2703−2734.

(4) Nitiss, J. L. DNA topoisomerase II and its growing repertoire of biological functions. *Nature Rev. Cancer* **2009**, *9*, 327−337.

(5) Nitiss, J. L. Targeting DNA topoisomerase II in cancer chemotherapy. *Natire Rev. Cancer* **2009**, *9*, 338−350.

(6) Champoux, J. J. DNA topoisomerases: structure, function, and mechanism. *Annu. Rev. Biochem.* **2001**, *70*, 369−413.

(7) Sundin, O.; Varshavsky, A. Arrest of segregation leads to accumulation of highly intertwined catenated dimers: dissection of the final stages of SV40 DNA replication. *Cell* **1981**, *25*, 659−669.

(8) Wilstermann, A. M.; Osheroff, N. Stabilization of eukaryotic topoisomerase II−DNA cleavage complexes. *Curr. Top. Med. Chem. (Hilversum, Neth.)* **2003**, *3*, 321−338.

(9) Vos, S. M.; Tretter, E. M.; Schmidt, B. H.; Berger, J. M. All tangled up: how cells direct, manage and exploit topoisomerase function. *Nature Rev. Mol. Cell Biol.* **2011**, *12*, 827−841.

(10) Baeyer, A. Ueber eine neue klasse von farbstoffen. *Ber. Dtsch. Chem. Ges.* **1871**, *4*, 555−558.

(11) Ueno, Y.; Jiao, G.-S.; Burgess, K. Preparation of 5- and 6-carboxyfluorescein. *Synthesis* **2004**, *2004*, 2591−2593.

(12) Cho, H. K.; Lone, S.; Kim, D. D.; Choi, J. H.; Choi, S. W.; Cho, J. H.; Kim, J. H.; Cheong, I. W. Synthesis and characterization of fluorescein isothiocyanate (FITC)-labeled PEO−PCL−PEO triblock copolymers for topical delivery. *Polymer* **2009**, *50*, 2357−2364.

(13) Onishi, H.; Machida, Y. Biodegradation and distribution of water-soluble chitosan in mice. *Biomaterials* **1999**, *20*, 175−182.

(14) Hoffmann, C.; Leroy-Dudal, J.; Patel, S.; Gallet, O.; Pauthe, E. Fluorescein isothiocyanate-labeled human plasma fibronectin in extracellular matrix remodeling. *Anal. Biochem.* **2008**, *372*, 62−71.

(15) Hattori, S.; Fujisaki, H.; Kiriyama, T.; Yokoyama, T.; Irie, S. Real-time zymography and reverse zymography: a method for detecting activities of matrix metalloproteinases and their inhibitors using FITC-labeled collagen and casein as substrates. *Anal. Biochem.* **2002**, *301*, 27−34.

(16) Liu, M.; Xie, C.; Pan, H.; Pan, J.; Lu, W. Separation of polyethylene glycols and their fluorescein-labeled compounds depending on the hydrophobic interaction by high-performance liquid chromatography. *J. Chromatogr., A* **2006**, *29*, 61−66.

(17) Teranishi, K.; Nishiguchi, T. Cyclodextrin-bound 6-(4-methoxyphenyl)imidazo[1,2-alpha±]pyrazin-3(7*H*)-ones with fluorescein as green chemiluminescent probes for superoxide anions. *Anal. Biochem.* **2004**, *325*, 185−195.

(18) Liu, J. M.; Huang, X. M.; Liu, Z. B.; Lin, S. Q.; Li, F. M.; Gao, F.; Li, Z. M.; Zeng, L. Q.; Li, L. Y.; Ouyang, Y. Exploitation of phosphorescent labelling reagent of fullerol−fluorescein isothiocyanate and new method for the determination of trace alkaline phosphatase as well as forecast of human diseases. *Anal. Chim. Acta* **2009**, *648*, 226−234.

(19) Hentz, N. G.; Richardson, J. M.; Sportsman, J. R.; Daijo, J.; Sittampalam, G. S. Synthesis and characterization of insulin−fluorescein derivatives for bioanalytical applications. *Anal. Chem.* **1997**, *69*, 4994−5000.

(20) Metallo, S. J.; Kane, R. S.; Holmlin, R. E.; Whitesides, G. M. Using bifunctional polymers presenting vancomycin and fluorescein groups to direct anti-fluorescein antibodies to self-assembled monolayers presenting D-alanine-D-alanine groups. *J. Am. Chem. Soc.* **2003**, *125*, 4534−4540.

(21) Puckett, C. A.; Barton, J. K. Fluorescein redirects a ruthenium−octaarginine conjugate to the nucleus. *J. Am. Chem. Soc.* **2009**, *131*, 8738−8739.

(22) Mills, C. O.; Milkiewicz, P.; Molloy, D. P.; Baxter, D. J.; Elias, E. Synthesis, physical and biological properties of lithocholyl−lysyl−fluorescein: a fluorescent monohydroxy bile salt analogue with cholestatic properties. *Biochim. Biophys. Acta* **1997**, *20*, 485−496.

(23) Yamana, K.; Mitsui, T.; Nakano, H. Synthesis and properties of oligonucleotide duplexes containing donor and acceptor fluorophores at 2′-positions. *Tetrahedron* **1999**, *55*, 9143−9150.

(24) Heyder, P.; Gaipl, U. S.; Beyer, T. D.; Voll, R. E.; Kern, P. M.; Stach, C.; Kalden, J. R.; Herrmann, M. Early detection of apoptosis by staining of acid-treated apoptotic cells with FITC-labeled lectin from *Narcissus pseudonarcissus*. *Cytometry, Part A* **2003**, *55*, 86−93.

(25) Nakayama, H.; Arakaki, A.; Maruyama, K.; Takeyama, H.; Matsunaga, T. Single-nucleotide polymorphism analysis using fluorescence resonance energy transfer between DNA-labeling fluorophore, fluorescein isothiocyanate, and DNA intercalator, POPO-3, on bacterial magnetic particles. *Biotechnol. Bioeng.* **2003**, *84*, 96−102.

(26) Dias, C. S.; Mitra, A. K. Vitreal elimination kinetics of large molecular weight FITC-labeled dextrans in albino rabbits using a novel microsampling technique. *J. Pharm. Sci.* **2000**, *89*, 572−578.

(27) Brush, C. K. Fluorescein labelled phosphoramidites. U.S. Patent US005583236A, 1994.

(28) Adamczyk, M.; Chan, C. M.; Fino, J. R.; Mattingly, P. G. Synthesis of 5- and 6-hydroxymethylfluorescein phosphoramidites. *J. Org. Chem.* **2000**, *65*, 596−601.

(29) Unciti-Broceta, A.; Diezmann, F.; Ou-Yang, C. Y.; Fara, M. A.; Bradley, M. Synthesis, penetrability and intracellular targeting of fluorescein-tagged peptoids and peptide−peptoid hybrids. *Bioorg. Med. Chem.* **2009**, *17*, 959−966.

(30) Singleton, S. F.; Roca, A. I.; Lee, A. M.; Xiao, J. Probing the structure of RecA−DNA filaments. Advantages of a fluorescent guanine analog. *Tetrahedron* **2007**, *63*, 3553−3566.

(31) Weatherman, R. V.; Kiessling, L. L. Fluorescence anisotropy assays reveal affinities of *C*- and *O*-glycosides for concanavalin A(1). *J. Org. Chem.* **1996**, *61*, 534−538.

(32) Natarajan, A.; Moerke, N.; Fan, Y. H.; Chen, H.; Christ, W. J.; Wagner, G.; Halperin, J. A. Synthesis of fluorescein labeled 7-methylguanosinemonophosphate. *Bioorg. Med. Chem. Lett.* **2004**, *14*, 2657−2660.

(33) Marchand, P.; Becerril-Ortega, J.; Mony, L.; Bouteiller, C.; Paoletti, P.; Nicole, O.; Barré, L.; Buisson, A.; Perrio, C. Confocal microscopy imaging of NR2B-containing NMDA receptors based on fluorescent ifenprodil-like conjugates. *Bioconjugate Chem.* **2011**, *23*, 21−26.

(34) Kierat, R. M.; Kramer, R. A fluorogenic and chromogenic probe that detects the esterase activity of trace copper(II). *Bioorg. Med. Chem. Lett.* **2005**, *15*, 4824−4827.

(35) Wang, H.; Li, J.; Liu, X.; Zhang, H.-S. *N*-Hydroxysuccinimidyl fluorescein-*O*-acetate as a highly fluorescent derivatizing reagent for aliphatic amines in liquid chromatography. *Anal. Chim. Acta* **2000**, *423*, 77−83.

(36) Uthirakumar, P.; Suh, E.-K.; Hong, C.-H.; Lee, Y.-S. Synthesis and characterization of polyesters containing fluorescein dye units. *Polymer* **2005**, *46*, 4640−4646.

(37) Du, X. L.; Zhang, H. S.; Deng, Y. H.; Wang, H. Design and synthesis of a novel fluorescent reagent, 6-oxy-(ethylpiperazine)-9-(2′-methoxycarbonyl) fluorescein, for carboxylic acids and its application in food samples using high-performance liquid chromatography. *J. Chromatogr., A* **2008**, *1178*, 92−100.

(38) Ge, F.-Y.; Chen, L.-G.; Zhou, X.-L.; Pan, H.-Y.; Yan, F.-Y.; Bai, G.-Y.; Yan, X.-L. Synthesis and study on hydrolytic properties of fluorescein esters. *Dyes Pigm.* **2007**, *72*, 322−326.

(39) Eshghi, H.; Mirzaie, N.; Asoodeh, A. Synthesis of fluorescein aromatic esters in the presence of P_2O_5/SiO_2 as catalyst and their hydrolysis studies in the presence of lipase. *Dyes Pigm.* **2011**, *89*, 120−126.
(40) Jing, B.; Zhu, D. Fullerene−fluorescein−anthracene hybrids: a model for artificial photosynthesis and solar energy conversion. *Tetrahedron Lett.* **2004**, *45*, 221−224.
(41) Crisp, G. T.; Millan, M. J. Conjugate addition of amino acid side chains to dyes containing alkynone, alkynoic ester and alkynoic amide linker arms. *Tetrahedron* **1998**, *54*, 649−666.
(42) Ying, L. Q.; Branchaud, B. P. Purification of tetracysteine-tagged proteins by affinity chromatography using a non-fluorescent, photochemically stable bisarsenical affinity ligand. *Bioconjugate Chem.* **2011**, *22*, 987−992.
(43) Chen, X.; Li, Z.; Xiang, Y.; Tong, A. Salicylaldehyde fluorescein hydrazone: a colorimetric logic chemosensor for pH and Cu(II). *Tetrahedron Lett.* **2008**, *49*, 4697−4700.
(44) Chen, X.; Ma, H. A selective fluorescence-on reaction of spiro form fluorescein hydrazide with Cu(II). *Anal. Chim. Acta* **2006**, *575*, 217−222.
(45) Li, T.; Yang, Z.; Li, Y.; Liu, Z.; Qi, G.; Wang, B. A novel fluorescein derivative as a colorimetric chemosensor for detecting copper(II) ion. *Dyes Pigm.* **2011**, *88*, 103−108.
(46) Zhang, L.; Zhang, X. A selectively fluorescein-based colorimetric probe for detecting copper(II) ion. *Spectrochim. Acta, Part A* **2014**, *133*, 54−59.
(47) Fujita, S.; Toru, T.; Kitagawa, Y.; Kagiyama, N.; Momiyama, M. Highly sensitive detection of membrane-bound DNA using fluorescein derivatives. *Anal. Chim. Acta* **1997**, *339*, 289−296.
(48) Adamczyk, M.; Mattingly, P. G.; Moore, J. A. *O*-(Fluoresceinylmethyl)hydroxylamine (OFMHA): a fluorescent reagent for detection of damaged nucleic acids. *Bioorg. Med. Chem. Lett.* **1998**, *8*, 3599−3602.
(49) Rukavishnikov, A. V.; Zaikova, T. O.; Birrell, G. B.; Keana, J. F.; Griffith, O. H. Synthesis of a new fluorogenic substrate for the continuous assay of mammalian phosphoinositide-specific phospholipase C. *Bioorg. Med. Chem. Lett.* **1999**, *9*, 1133−1136.
(50) Mugherli, L.; Burchak, O. N.; Chatelain, F.; Balakirev, M. Y. Fluorogenic ester substrates to assess proteolytic activity. *Bioorg. Med. Chem. Lett.* **2006**, *16*, 4488−4491.
(51) Chen, L.; Li, F. Q.; Hou, B. H.; Hong, G. F.; Yao, Z. J. Site-specific fluorescent labeling approaches for naringenin, an essential flavonone in plant nitrogen-fixation signaling pathways. *J. Org. Chem.* **2008**, *73*, 8279−8285.
(52) Huang, Y.-J.; Wang, H.; Gao, F.-B.; Li, M.; Yang, H.; Wang, B.; Tai, P. C. Fluorescein analogues inhibit SecA ATPase: the first submicromolar inhibitor of bacterial protein translocation. *ChemMedChem* **2012**, *7*, 571−577.
(53) Marini, J. C.; Miller, K. G.; Englund, P. T. Decatenation of kinetoplast DNA by topoisomerases. *J. Biol. Chem.* **1980**, *255*, 4976−4979.
(54) Deane, F. M.; O'Sullivan, E. C.; Maguire, A. R.; Gilbert, J.; Sakoff, J. A.; McCluskey, A.; McCarthy, F. O. Synthesis and evaluation of novel ellipticines as potential anti-cancer agents. *Org. Biomol Chem.* **2013**, *11*, 1334−1344.
(55) Wilson, C. R.; Fagenson, A. M.; Ruangpradit, W.; Muller, M. T.; Munro, O. Q. Gold(III) complexes of pyridyl- and isoquinolylamido ligands: structural, spectroscopic, and biological studies of a new class of dual topoisomerase I and II inhibitors. *Inorg. Chem.* **2013**, *52*, 7889−7906.
(56) Park, H. J.; Lee, H. J.; Lee, E. J.; Hwang, H. J.; Shin, S. H.; Suh, M. E.; Kim, C.; Kim, H. J.; Seo, E. K.; Lee, S. K. Cytotoxicity and DNA topoisomerase inhibitory activity of benz[*f*]indole-4,9-dione analogs. *Biosci., Biotechnol., Biochem.* **2003**, *67*, 1944−1949.
(57) Bandele, O. J.; Osheroff, N. The efficacy of topoisomerase II-targeted anticancer agents reflects the persistence of drug-induced cleavage complexes in cells. *Biochemistry* **2008**, *47*, 11900−11908.
(58) Neto, B. A.; Lapis, A. A. Recent developments in the chemistry of deoxyribonucleic acid (DNA) intercalators: principles, design, synthesis, applications and trends. *Molecules* **2009**, *14*, 1725−1746.
(59) Vance, J. R.; Bastow, K. F. Inhibition of DNA topoisomerase II catalytic activity by the antiviral agents 7-chloro-1,3-dihydroxyacridone and 1,3,7-trihydroxyacridone. *Biochem. Pharmacol.* **1999**, *58*, 703−708.
(60) Franken, N. A.; Rodermond, H. M.; Stap, J.; Haveman, J.; van Bree, C. Clonogenic assay of cells in vitro. *Nature Protoc.* **2006**, *1*, 2315−2319.
(61) Baviskar, A. T.; Madaan, C.; Preet, R.; Mohapatra, P.; Jain, V.; Agarwal, A.; Guchhait, S. K.; Kundu, C. N.; Banerjee, U. C.; Bharatam, P. V. N-Fused imidazoles as novel anticancer agents that inhibit catalytic activity of topoisomerase IIalpha and induce apoptosis in G1/S phase. *J. Med. Chem.* **2011**, *54*, 5013−5030.
(62) Kuang, H. B.; Miao, C. L.; Guo, W. X.; Peng, S.; Cao, Y. J.; Duan, E. K. Dickkopf-1 enhances migration of HEK293 cell by beta-catenin/E-cadherin degradation. *Front. Biosci.* **2009**, *14*, 2212−2220.
(63) Dantzer, F.; Schreiber, V.; Niedergang, C.; Trucco, C.; Flatter, E.; De La Rubia, G.; Oliver, J.; Rolli, V.; Menissier-de Murcia, J.; de Murcia, G. Involvement of poly(ADP-ribose) polymerase in base excision repair. *Biochimie* **1999**, *81*, 69−75.
(64) Toyoshima, H.; Hunter, T. P27, a novel inhibitor of G1 cyclin-Cdk protein kinase activity, is related to p21. *Cell* **1994**, *78*, 67−74.
(65) Zi, X.; Feyes, D. K.; Agarwal, R. Anticarcinogenic effect of a flavonoid antioxidant, silymarin, in human breast cancer cells MDA-MB 468: induction of G1 arrest through an increase in Cip1/p21 concomitant with a decrease in kinase activity of cyclin-dependent kinases and associated cyclins. *Clin. Cancer Res.* **1998**, *4*, 1055−1064.
(66) Lohse, J.; Nielsen, P. E.; Harrit, N.; Dahl, O. Fluorescein-conjugated lysine monomers for solid phase synthesis of fluorescent peptides and PNA oligomers. *Bioconjugate Chem.* **1997**, *8*, 503−509.
(67) Jun, K. Y.; Kwon, H.; Park, S. E.; Lee, E.; Karki, R.; Thapa, P.; Lee, J. H.; Lee, E. S.; Kwon, Y. Discovery of dihydroxylated 2,4-diphenyl-6-thiophen-2-yl-pyridine as a non-intercalative DNA-binding topoisomerase II-specific catalytic inhibitor. *Eur. J. Med. Chem.* **2014**, *80*, 428−438.
(68) Park, S. H.; Park, S. J.; Kim, J. O.; Shin, J. H.; Kim, E. S.; Jo, Y. K.; Kim, J. S.; Jin, D. H.; Hwang, J. J.; Lee, S. J.; Jeong, S. Y.; Lee, C.; Kim, I.; Cho, D. H. Down-regulation of survivin by nemadipine-a sensitizes cancer cells to trail-induced apoptosis. *Biomol. Ther.* **2013**, *21*, 29−34.
(69) Park, S. E.; Chang, I. H.; Jun, K. Y.; Lee, E.; Lee, E. S.; Na, Y.; Kwon, Y. 3-(3-Butylamino-2-hydroxy-propoxy)-1-hydroxy-xanthen-9-one acts as a topoisomerase IIalpha catalytic inhibitor with low DNA damage. *Eur. J. Med. Chem.* **2013**, *69*, 139−145.
(70) Joung, K. E.; Min, K. N.; Kim, D. K.; Sheen, Y. Y. Anti-cancer effect of IN-2001 in T47D human breast cancer. *Biomol. Ther.* **2012**, *20*, 81−88.